

# Acoustics Development for Exhaust Gas Turbochargers

The increasing application of turbocharged engines shifts turbocharger acoustics more into the focus of development. Here the noise behaviour of the turbocharger provides a conflict between costs and acoustics. In the context of the FVV research project No 866 "Turbo Charger Noise" the noise behaviour of turbochargers was subjected to systematic experimental investigations and a hybrid simulation methodology was developed at the institute for combustion engines (VKA) of the RWTH Aachen. The good conformity of calculation and measurement ensures the characterization of the acoustical behaviour and implementation of acoustical measures in the layout of the turbocharger early in the development process. Thus cost-intensive rework can be avoided at the end of the development process.

## 1 Introduction

The rising performance requirements of modern supercharged diesel engines and the trend to supercharged direct injection gasoline engines constitute a set of acoustic risks for the developers concerning the turbocharger calibration. Today the acoustic optimization is based exclusively on empirical models to describe the noise behaviour of turbochargers. The extensive mechanisms of noise generation and their dependency speak for the necessity of an efficient simulation-based calculation tool, which can be used in an early stage of the development process.

In most cases the disturbing noise caused by the turbocharger is not relevant for the overall level of the engine. Its tonal character is commonly pronounced in a frequency range higher than 500 Hz and thus outside the level-determining frequency range. This leads to an intensified perception by humans. Especially characteristic noises must also be regarded in the context with the expectations of the driver. Under low-speed part load operation such noises could be annoying or even be characterized as malfunction [1]. On the other hand, however, a slight whistling could be perceived quite pleasantly by the driver. This can be the case when the engine is operated at high speed and full load since it is a direct acoustic feedback of the power output of the engine.

This generates a lot of requirements on a development tool whereby the different gas and rotor dynamic excitation sources of the turbocharger need to be represented appropriately over the com-

plete speed range. In addition, the structure-borne noise propagation in the involved engine components is to be considered. In the context of an FVV research project a two-stage approach was carried out: first, measurements were conducted while doing extensive parameter variations on the exhaust gas turbochargers (TC) of a passenger car engine and a heavy duty engine in order to characterise the different noise phenomena caused by the particular applications and to quantify the individual dominating factors of the acoustics of the turbocharger. Secondly, a hybrid computation method has been developed based on flow, multi-body and dynamic finite-element simulation. It was revealed that the obtained result correlates very well with the experimental data. Thus the individual results will contribute significantly to further understanding of the complex acoustic mechanisms of a turbocharger and allow for a virtual layout of the turbocharger system.

## 2 Experimental Investigation

Subsequently, test engines, noise phenomena, and influencing factors are described regarding the experimental investigations.

### 2.1 Test Engines

The experimental investigations were performed using either a passenger car engine or a truck engine. The basic work scope was acceleration measurements at the turbocharger, measurements of the pressure pulsations in the exhaust and intake system, and airborne noise meas-

**Table:** Technical information of the test engines

Engine	Passenger car	Truck
Injection / fuel type	DI / Diesel	DI / Diesel
Cylinder configuration	Inline 4	Inline 6
Displacement / bore / stroke	1,4 l / 73,7 mm / 82,0 mm	10,5 l / 120 mm / 155 mm
Nominal power	50 kW @ 4000 rpm	316 kW @ 1900 rpm
Turbocharger concept	Waste gate	EGR bypass
Max. turbocharger speed	240,000 rpm	115,000 rpm
Number of blades turbine / compressor	T. 9 / C. 5 and 5 splitter	T. 11 / C. 7 and 7 splitter
Typical noise phenomena range	1000 – 18,000 Hz	500 – 13,000 Hz

## Authors



**Prof. Dr.-Ing. Stefan Pischinger** is director of the Institute for Combustion Engines (VKA) of Aachen University of Technology (RWTH Aachen) (Germany).



**Dr.-Ing. Harald Stoffels** was the chairman of the FVV project; he is in charge of Acoustics and Dynamics within the Gasoline Powertrain R&D department and is affiliated to Ford Werke GmbH, Cologne (Germany).



**Dr.-Ing. Christoph Steffens** is department manager vehicle physics / acoustic of FEV Motorentechnik GmbH in Aachen (Germany).



**Dipl.-Ing. Richard Aymanns** is scientific assistant at the Institute for Combustion Engines (VKA) of Aachen University of Technology (RWTH Aachen) (Germany).



**Dipl.-Ing. Rémi Stohr** is engineer in the department vehicle physics / acoustic of FEV Motorentechnik GmbH in Aachen (Germany).



**Dipl.-Ing. Martin Atzler** is scientific assistant at the Institute for Combustion Engines (VKA) of Aachen University of Technology (RWTH Aachen) (Germany).

urements under anechoic conditions. The **Table** shows the specifications of the individual engines and turbochargers investigated.

2.2 Noise Phenomena

The occurring noise phenomena of the investigated turbochargers can be divided in four acoustical phenomena caused by different physical effects. These four phenomena can be perceived as noises of a tonal character. In **Figure 1** the characteristics of the different phenomena are displayed in the form of Campbell diagrams for both investigated engines.

The constant-tone is different from the other three noise phenomena, because its related frequency is not proportional to the turbocharger-speed. After a slight increasing slope at low TC-speed the tone is associated with a constant frequency versus rotor-speed. This frequency is defined by the lateral bending vibra-

tion of the TC-shaft in the hydro dynamical oil film of the journal-bearings of the rotor. For the passenger car TC typical values are in the range of 1000 Hz, and for the truck TC around 500 Hz.

Another phenomena can be the unbalancing whistle. Because of high rotor speeds, large unbalancing forces can occur in turbocharger systems. These rotating forces are linearly proportional to the frequency of the turbocharger-speed and cause a tonal noise, commonly known as unbalancing whistle [2]. The frequency range of the unbalancing whistle extends up to 4 kHz for the passenger car engine investigated and up to 2 kHz with the truck engine.

Like the unbalancing whistle the pulsation noise occurs with the rotation frequency of the turbocharger rotor. Physical causes of this phenomenon are rotor asymmetries, which lead to alternating forces when the irregularities

are rotating relative to the non-moving housing.

The rotating noise is caused by the pressure difference between pressure and suction side of the particular rotor blades and by the blades passing the housing tongue. The frequency of the excitation is determined by the product of the TC-speed and the number of blades of the turbine respectively compressor wheel [3]. Because of the high turbocharger-speed of the passenger car TC of up to 240,000 rpm and five vanes at the compressor- and nine blades at the turbine-wheel, its rotating noise lies mainly above the audible range. Therefore this phenomenon plays a subordinate role in the investigation. With the essential larger TC of the truck engine the rotating noise lies due to its lower rotation speed in the frequency range of up to 13 kHz, which can be clearly perceived under full-load condition.

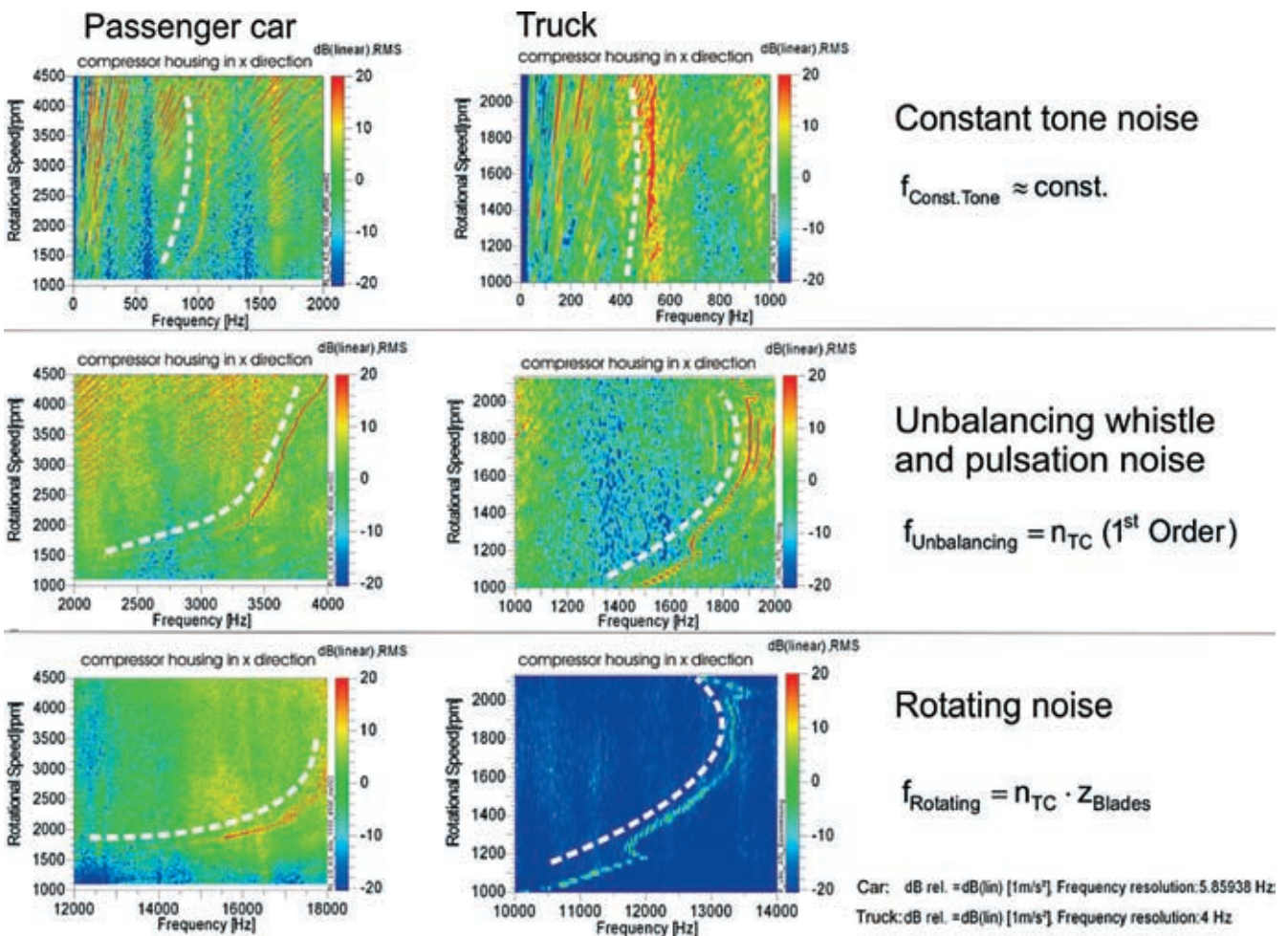


Figure 1: Structure born noise measurement: depiction of turbo charger noise phenomena

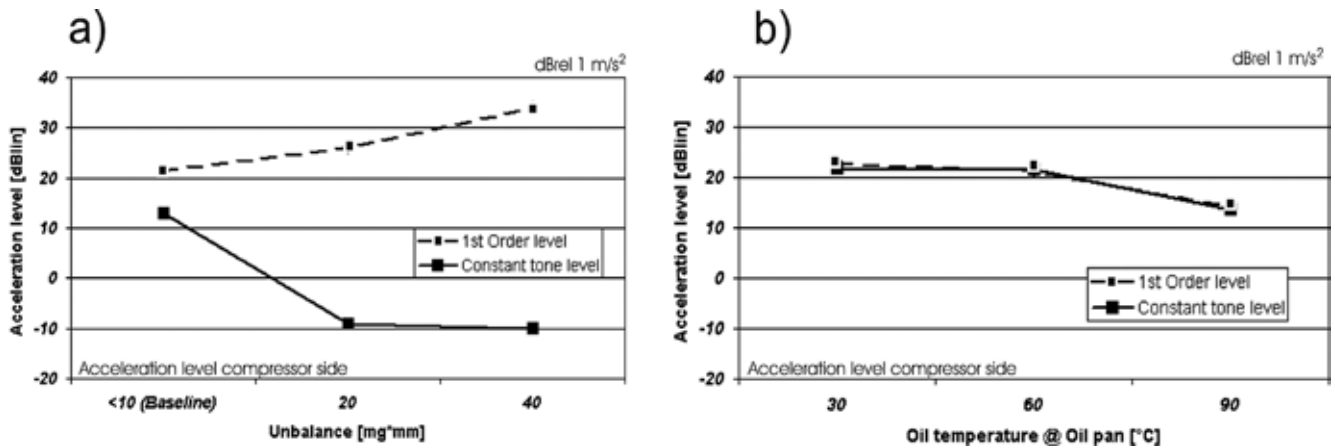


Figure 2: Influence on structure born noise behaviour of the turbo charger due to unbalance (a) and oil temperature (b)

### 2.3 Influencing Factors

Based on measurements of the passenger car engine under fired operation, the influencing factors of various layout-parameters can be associated to the individual noise phenomena. The acceleration levels displayed in Figure 2 were measured at the compressor side of the TC at 200,000 rpm. In addition the noise share of the several noise phenomena was considered separately. This was on one hand the constant-tone (band pass from 900 to 1100 Hz), and on the other hand the unbalancing whistle and pulsation noise (first TC-order).

#### 2.3.1 Influence of the Unbalance

With grub screws on the compressor side an unbalance was added to the remaining unbalance caused by already existing manufacturing tolerance ranges. Two turbochargers with an additional mass of 20 and 40 mg were tested. As expected, Figure 2a shows a clear dependency of the level of the unbalancing whistle to the applied mass. Here the level of the first order follows considered unbalance in a linear rising shape. The constant-tone values on the contrary are so low from 20 mg unbalance upwards that this noise phenomenon can be considered as not detectable.

#### 2.3.2 Influence of the Oil Temperature

The oil temperature was changed in the range from 30 to 90 °C (in the oil pan) to investigated the influence of the oil temperature and therefore the oil viscosity on turbocharger noise, Figure 2b. The excitation of the first turbocharger or-

der and the constant-tone show a graduate level reduction with increasing oil temperature.

Besides the displayed influence on the first order level, the higher oil temperature also leads to a small shift of the constant-tone to lower frequencies. This effect can be explained by the alternating damping effect of the hydrodynamic bearing on the natural vibration behaviour of the TC-rotor, due to the oil viscosity variation.

#### 2.3.3 Influence of the Air Inflow

For the investigated truck turbocharger, a so-called noise-ring was applied in order to reduce the rotating noise. The effect of the noise-ring on the dominance of the rotating noise was shown with a comparative measurement where the noise-ring was removed. The noise-ring achieves an

improvement potential of up to 10 dB on the first order level under full load condition in the middle speed range.

## 3 Hybrid Simulation Method

A multidisciplinary CAE model was developed in order to analyse the mechanisms of noise generation and to investigate their influence by performing detailed parametric studies. The structure and the interfaces between the separate calculation methods are depicted in Figure 3. The first part contains the gas flow simulation (CFD). Results of the CFD simulation are pressure pulsations of the gas flow, which on one hand directly lead to airborne noise and on the other hand cause a force excitation on the rotor. The forces on the rotor are used as a boundary

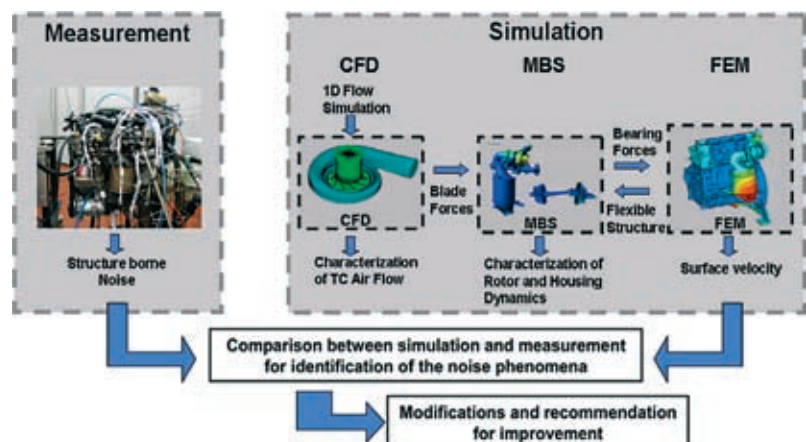


Figure 3: Structure of the CAE model for the analysis of noise generation and transfer of the turbocharger

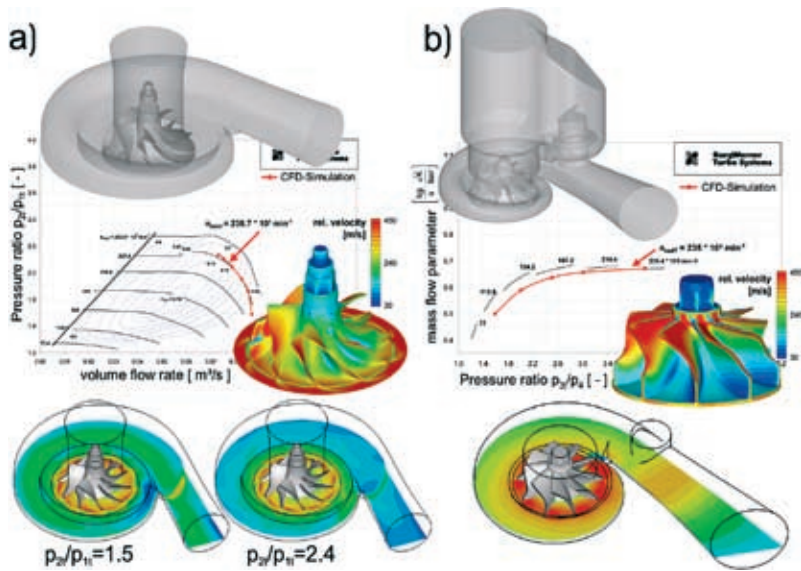


Figure 4: Validation of the CFD models for compressor (a) and turbine (b) with measured maps

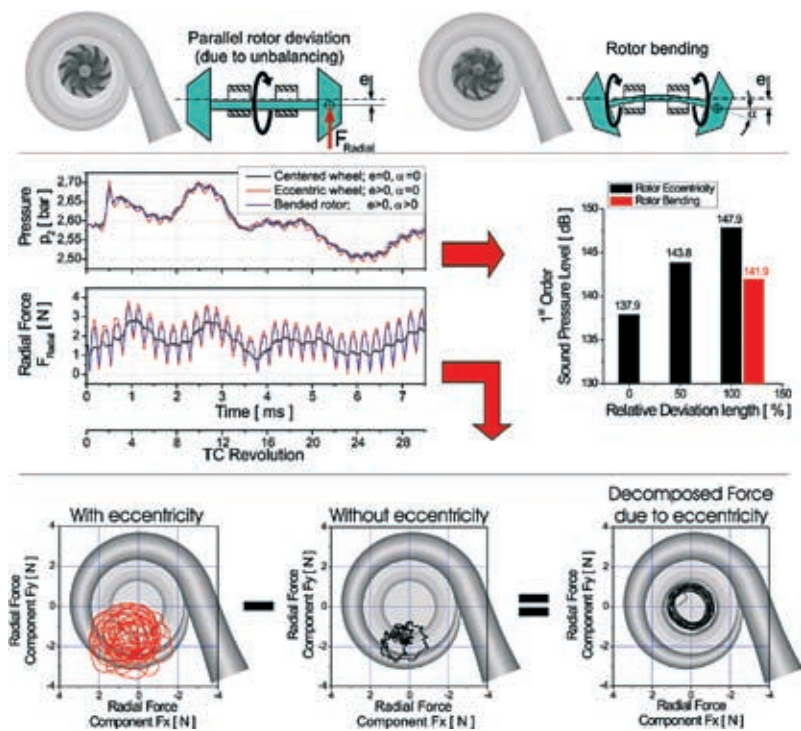


Figure 5: Results of the CFD calculation at different rotor deviations

condition for the second part, the multi body simulation (MBS). From the MBS calculations, bearing forces can be extracted as a result of the description of the rotor dynamics. The bearing forces are then used as an excitation for the third part, the analysis of the dynamic structure response (FEM). Finally, the forced-response results of the engine can be compared to

measurement results of the engine in order to validate the calculation.

### 3.1 CFD Simulation

The gas-flow-dynamics in turbine and compressor is calculated based on a three-dimensional gas dynamic simulation (CFD) using the software Star-CD. Target is to investigate the influence of a

deviation of the turbine and compressor wheel on the pressure excitation of the gas flow, and on the resulting gas forces acting on the wheels. Furthermore, the gas forces are used as an input for the multi body simulation in order to calculate the structure excitation caused by the gas flow. The wheel deviation can be separated into a purely parallel offset in the bearing clearance, caused by unbalance, and into an angular deviation, caused by bending of the rotor. Both deviations are rotating with the rotor speed, as is depicted schematically in the top of Figure 5.

The flow region covered by the CFD calculation contains scroll, wheel, inlet and outlet of compressor and turbine respectively. The computational grids consist of about 1 million cells for the compressor and 3 million cells for the turbine, Figure 4.

Steady state simulations of particular points of operation within the performance map show a good correlation to the measured maps of turbine and compressor, Figure 4. The flow field at the impeller outlet of the compressor exhibits a clear dependency on the back pressure. With increasing back pressure the mean outlet mass flow is shifted towards the start of the scroll, which leads to an uneven load and thus evokes a radial force on the wheel.

For the acoustic assessment transient flow simulations were performed to resolve the pressure and force oscillation. The motion of the wheels in terms of rotation was realized by a moving mesh. At the borders of the area considered for the calculation, pressure and mass flow rate traces as well as temperatures are applied as boundary conditions. These boundaries were taken from one dimensional gas exchange calculations.

Figure 5 shows the evaluation of the simulation results for the compressor, comparing a centered arrangement with two different rotor deviations. The force and pressure for the centered rotor show a clear coherence between radial force on the impeller and pressure after compressor  $p_2$ , which can be explained by the shift of the mean outlet flow as described before.

The radial forces gained from the simulation of the variants with eccentric rotor show an excitation of the first turbo-

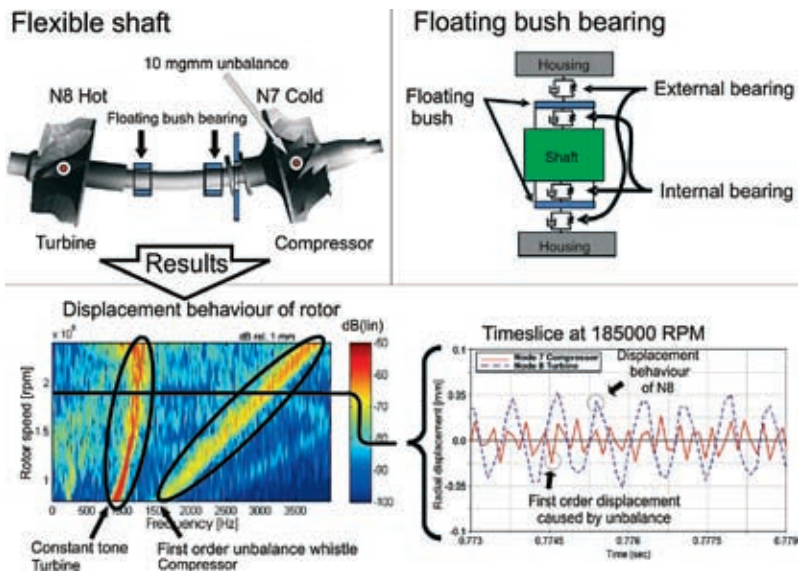


Figure 6: MBS model setup and evaluation of calculated rotor displacement

charger order with an amplitude of about 1 N. Here, the mean trend follows exactly the one for a centered rotor. From this a complete separation of the force excitation caused by boundary conditions and wheel deviation can be inferred (Figure 5, bottom). The excitation amplitude due to eccentricity shows only a marginal effect of the boundary condition, but depends linearly on the amount of deviation. However, the force excitation caused by the gas flow is negligible low in comparison to the dynamic bearing forces calculated by the multi body simulation.

Acoustically more remarkable than the radial force are the post-compressor pressure characteristics,  $p_2$ . Similar to the description of the radial force, a wheel deviation causes an excitation of the first turbocharger order, which is superimposed on the pressure trace induced by the engine operation. Also here the deviation length has a significant impact, as is shown in Figure 5 on the right side. A deviation of 100 % corresponds to the full bearing clearance. The variant with a bended rotor (red bar) shows a slightly different behaviour. The eccentricity  $e$  of the impeller, which is even larger than with purely parallel deviation, also causes a pressure excitation. This is, however, clearly reduced by the additional angle  $\alpha$ . Reason for that is the tip clearance between rotor blades and housing, which becomes larger within the range of the rotor outlet due to this

angle. At the compressor especially this region plays an important role for the load transfer onto the gas flow, so that the increased gap leads to a decrease of the pressure excitation.

On the turbine side, a similar correlation is found between impeller eccentricity and the excitation of pressure and force similar as at the compressor. Different with the compressor the bending angle " $\alpha$ " has almost no effect on the turbine side, so that an additional eccentricity due to rotor bending directly increases the amplitude of the pressure excitation. In total the amplitudes of force and pressure pulsation on the turbine side are significantly lower than on the compressor side.

It can be summarized that an impeller eccentricity primarily leads to airborne noise dominated by the first turbocharger order, whereas the level of the excitation by the forces acting on the rotor are negligibly small. On the compressor side, which is clearly more susceptible to this phenomenon, the noise excitation is again reduced by a bending of the rotor.

### 3.2 MBS Simulation

The intention of an MBS simulation is to simulate the system behaviour of coupled bodies. As a result, forces, moments, displacements, velocities and accelerations can be evaluated to analyse the system behaviour. In order to be able to calculate a realistic simulation behaviour it

is necessary to implement the coupling conditions of the bodies and consider the correct phase of external forces, moments and motion specifications, besides the properties of the considered bodies. The rotor is a crucial element of the investigated system. As already mentioned, the rotor rotates at very high speeds, which lead to high mass forces. In the used commercial software Adams/Engine, bearing elements exist with hydrodynamical properties, which solve the Reynolds equation considering bearing-geometry, bearing-clearance, temperature and oil viscosity for each simulation time step [4]. A speciality of the considered turbocharger is the floating bush bearing of the rotor. This bearing features two into each other supporting hydro-dynamical bearings, which are coupled by a floating bush.

The rotor as well as the housing are integrated in the model as a flexible body. In Figure 6 the principle set-up of the MBS model is depicted.

A run-up simulation is performed with the baseline turbo charger, from 0 to 240,000 rpm, including a remaining unbalance at the rotor. The system behaviour will be analysed based on the displacement of the rotor relative to the housing. For identifying the phenomena, a conversion of the time signals into the frequency domain depicted in a Campbell diagram has proved to be the best way to evaluate the simulation. When considering the rotor displacement two significant phenomena can be observed:

1. A dominant first rotor order, which is caused by the unbalance of the rotor.
2. A half order, which changes into a constant frequency, also known as constant-tone.

The root cause mechanism of the constant-tone is based on two different effects: in the half order-dominating speed range up to 60,000 rpm the rotor rolls within the clearance of the hydrodynamic bearing. This roll speed is affected by the characteristics of the oil and the axial clearance. This roll speed is clearly lower than the rotational speed of the rotor. The transition to the resonant frequency is initiated when the roll speed coincide with the bending-critical overspeed of the rotor. In Figure 6 the displacement behaviour of the shaft is represented, where the time slice shows a

different behaviour of the two shaft ends. A bending of the shaft on the turbine side dominates the behaviour concerning the constant-tone, while on the compressor side the unbalance causes unbalancing whistle.

For the verification of the MBS model calculations of different variants were performed, and compared with the corresponding measurement results. One of the variants was a reduction of the oil viscosity which was examined by increasing the oil temperature. In both, measurement and calculation a reduction of the constant-tone frequency can be observed. Furthermore, the influence of a larger unbalance of 40 mgmm on the compressor side was investigated. The result is a significant increase of the first TC-order with simultaneously a reduction of the constant-tone level. Both noise phenomena are well pronounced, as the comparison with the measurements displays in **Figure 7**.

Further calculation steps had the goal to reach a minimisation of the individual noise phenomena without a degradation of the responsiveness of the rotor itself. Variants could be achieved with which an acoustic improvement was to be expected, however the feasibility of some variants must be investigated regarding further criteria.

### 3.3 FE Calculation

Finally, by finite element simulation with the commercial software Ansys the gas forces extracted from the CFD analysis and the bearing reaction forces from the MBS simulation are loaded on the housing structure in a forced-response calculation. As a result the structural answer and the associated surface mobility are obtained, Figure 7.

The calculation takes place in the time domain so that phase relationships of the individual force components can be considered. A first step in this calcula-

tion methodology is the modal analysis, which determines the natural frequencies of the structure. The natural frequencies for this model were calculated up to a frequency range of 4.5 kHz. This was done in order to observe the expected effects of the individual turbocharger's noise phenomena. In the second step the forces and moments extracted from the MBS simulation including the gas forces of the CFD analysis are loaded in the corresponding areas of the turbocharger housing, and finally the structure answer was calculated. It was found that the surface dynamics are dominated primarily by the motion behaviour of the shaft and the force excitation caused by the flow is of subordinated importance. Due to the simulation in the time domain the results of the calculation can be represented in a Campbell diagram, as is shown in **Figure 8**.

In a further step the transfer path of the complete engine structure was deter-

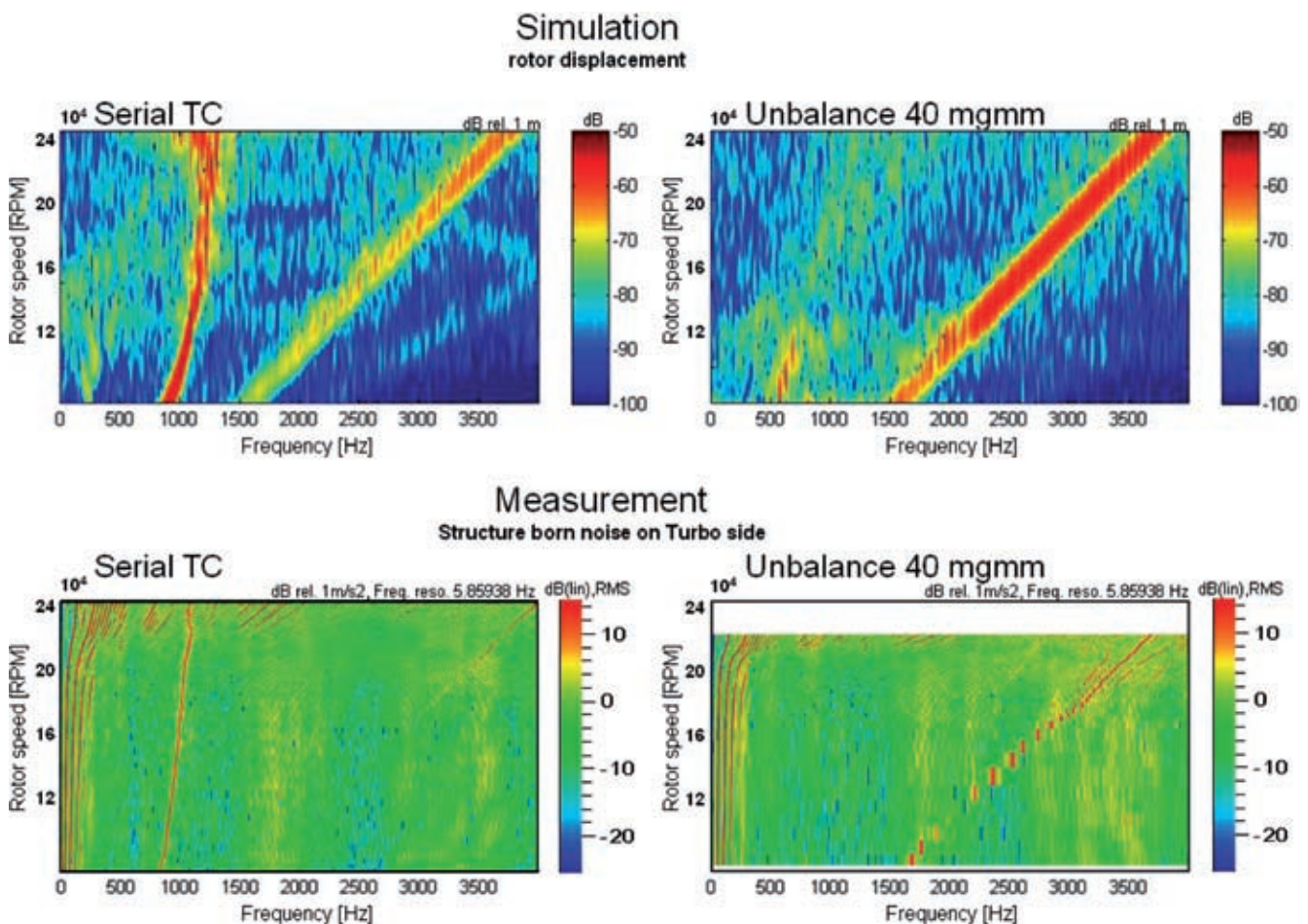


**Figure 7:** Comparison simulation versus measurement: influence of unbalance

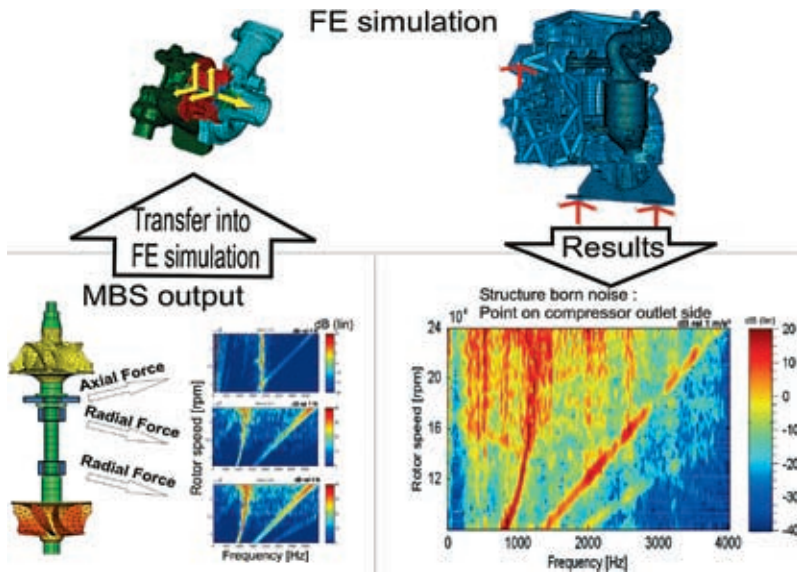


Figure 8: Setup of FE model and calculated structure acceleration at compressor outlet

mined. In Figure 9 the surface velocity sumlevel of the individual components is represented, for a frequency range of up to 4000 Hz. The simulation shows that the turbocharger housing and the elbow between turbine outlet and catalyst are the dominant components with respect to the turbocharger noise.

#### 4 Summary

A fundamental understanding of turbocharger noise phenomena was obtained

by the described analyses of experimental testing and calculations in this article of the FVV research project “Turbo Charger Noise” at the institute for combustion engines (VKA) of the RWTH Aachen. The presented simulation method enables an acoustically refined design of the turbocharger in the early development process. To represent the complex excitations and transfer paths sufficiently in detail, an interdisciplinary concept was developed. It is based on a combination of the simulations of flow dynamics (CFD), rotor dynamics

**Acknowledgements**  
 This article is a summary of the results of a research project assigned by Forschungsvereinigung Verbrennungskraftmaschinen e. V. (FVV, Frankfurt/Main, Germany) and conducted at the Institute for Combustion Engines of Aachen University of Technology (RWTH Aachen) under the supervision of Prof. Stefan Pischinger. The work was funded by FVV own resources. The project was supported by a work group of FVV under the supervision of Dr. Harald Stoffels, Ford-Werke GmbH. We thank the work group and especially Dr. Stoffels for their considerable help. We would also like to thank the companies Ford-Werke GmbH, MAN Nutzfahrzeuge AG and especially BorgWarner Turbo Systems GmbH for the great support.

(MBS) and dynamic structure transfer (FEM). The quality of the calculation model was verified with measurements obtained from the complete engine of a small-passenger vehicle and a commercial vehicle. Apart from the occurrence of the phenomena the influence of bearing specification can be described with such an approach.

#### References

- [1] Stoffels, H.; Schroerer, M.: NVH Aspects of a Downsized Turbocharged Gasoline Powertrain with Direct Injection. Transactions of the SAE 2003. SAE N&V Conference 2003, Traverse City, MI. SAE Paper No. 2003-01-1664. Warrendale, 2003
- [2] Klaus, B.; Krieger, E.: The Influence of Modern Turbochargers on the Acoustics of Exhaust Systems for Direct Injection Diesel Engines. Transaction of the 20th International Vienna Engine Symposium, 6–7 May 1999
- [3] Schachner, P.; Reisinger, W.: Akustische Optimierung von Abgasturboladern für PKW-Dieselfahrzeuge. VDI-Berichte, Heft 910, S. 297–314, Düsseldorf, 1991
- [4] Rebbert, M.: Simulation der Kurbelwellendynamik unter Berücksichtigung der hydrodynamischen Lagerung zur Lösung motorakustischer Fragen. Dissertation, RWTH Aachen, 2000
- [5] El Tahry, S.H.:  $K, \epsilon$  – Equation for Compressible Reciprocating Engine Flows. In: AIAA J Energy, 1983, 7 (4), pp 345–353
- [6] Kreuz-Ihli, T.; Filsinger, D.; Schulz, A.; Wittig, S.: Numerical and Experimental Study of Unsteady Flow Field and Vibration in Radial Inflow Turbines. Journal of Turbomachinery, April 2000, Vol. 122/247

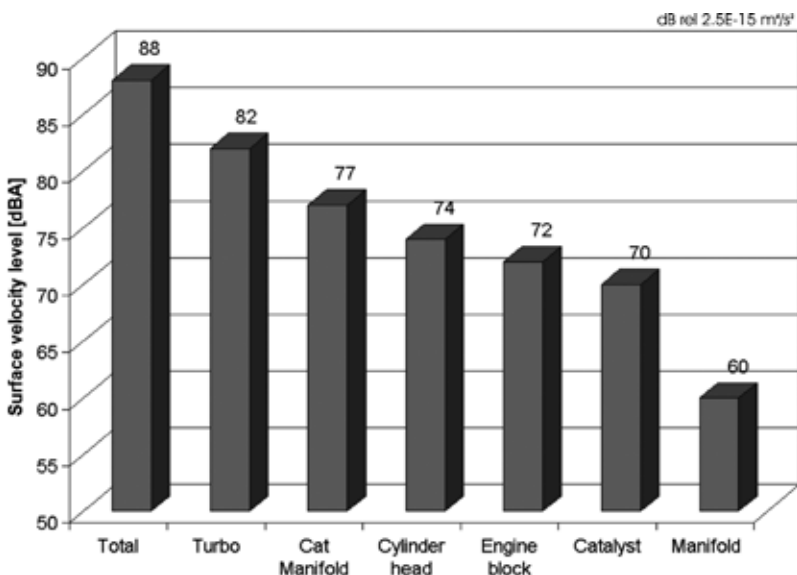


Figure 9: Surface velocity sumlevel for the separate engine components